A rice high-affinity potassium transporter (HKT) conceals a calcium-permeable cation channel

Wen-Zhi Lan[a], Wei Wang[b,c], Suo-Min Wang[a,d], Le-Gong Li[a,e], Bob B. Buchanan[a,1], Hong-Xuan Lin[b,c], Ji-Ping Gao[b,c], and Sheng Luan[a,c,1]

[a]Department of Plant and Microbial Biology, University of California, Berkeley, CA 94720; [b]National Key Laboratory of Plant Molecular Genetics, Institute of Plant Physiology and Ecology, Shanghai Institutes for Biological Sciences, Chinese Academy of Sciences, Shanghai 200032, China; [c]Shanghai Institutes for Biological Sciences–Univerisity of California Berkeley Center for Molecular Life Sciences, Shanghai 200032, China; [d]School of Pastoral Agriculture Science and Technology, Key Laboratory of Grassland Agro-ecosystem, Ministry of Agriculture, Lanzhou University, Lanzhou 730000, China; and [e]College of Life Sciences, Capital Normal University, Beijing 100037, China

Contributed by Bob B. Buchanan, January 22, 2010 (sent for review November 10, 2009)

Plant high-affinity K^+ transport (HKT) proteins are so named because of their relation to bacterial and fungal transporters that mediate high-affinity K^+ uptake. The view that HKT family members are sodium-selective uniporters or sodium-potassium symporters is widely held. We have found that one of the rice HKT proteins also functions as a Ca^{2+}-permeable cation channel that conducts current carried by a wide range of monovalent and divalent cations. The *HKT* rice gene, named *OsHKT2;4,* is expressed in several cell types, including root hairs and vascular parenchyma cells. The protein is localized to the plasma membrane, thereby providing a mechanism for cation uptake and extrusion. This finding goes against firmly entrenched dogma in showing that HKT proteins can function as both ion carriers and channels. The study further extends the function of HKT proteins to Ca^{2+}-linked processes and, in so doing, defines a previously undescribed type of Ca^{2+}-permeable cation channels in plants. The work also raises questions about the evolutionary changes in this protein family following the divergence of monocots and dicots.

calcium transport | moncot–dicot divergence | nonselective cation channel

On the basis of a comparative structural analysis, plant HKTs (for high-affinity K^+ transport) appear to be homologous to a family of bacterial and fungal K^+ transporters, including Ktr proteins in *Vibrio alginolyticus* (1) and TRKs in yeast (2, 3). All of these proteins facilitate high-affinity K^+ uptake (1, 3). The plant HKTs differ, however, in their ability to act as both Na^+ uniporters and Na^+-K^+ symporters (4–8). Despite this functional diversity, all Ktr/TRK/HKT family members are predicted to contain eight transmembrane domains that could form four membrane-pore-membrane motifs reminiscent of the pore domain in the KcsA K^+ channel (9, 10). On the basis of differences in their amino acid sequences and transport properties, wheat HKT1 and *Arabidopsis* AtHKT1;1 represent two distinct groups of proteins (11). Group 1, represented by *Arabidopsis* AtHKT1;1, contains a serine in the first p-loop of the four-pore domain structure and selectively transports Na^+. Group 2, typified by wheat HKT1, on the other hand, has glycine in place of serine and acts as a symporter for both Na^+ and K^+.

Compared with a single *AtHKT1;1* gene in the dicot model, *Arabidopsis*, rice, a monocot model, contains nine *HKT*-like genes (12), a striking departure from *Arabidopsis*. Available data suggest that various members within the rice HKT family may belong to either group 1 or to group 2 HKTs (13, 14). A recent study identified the *OsHKT1;5* gene that serves as a critical quantitative trait locus for salt tolerance in rice because this gene product functions as a Na^+-specific transporter as AtHKT1;1 does (5). A second *HKT* gene in rice (*OsHKT2;1*) was shown to take up Na^+ to maintain cell growth under low-K^+ conditions (15).

Here we present evidence that, surprisingly, a HKT member of group 2 in rice acts as a channel for the transport of both mono- and divalent cations, e.g., Ca^{2+} and Mg^{2+}. In extending the function of the HKT protein family to Ca^{2+} transport, these findings raise the questions of how HKT proteins participate in Ca^{2+} signaling and how this functional divergence occurred between monocots and dicots.

Results and Discussion

OsHKT2;4 Protein Expressed in *Xenopus* Oocytes Produces a Unique Cation Current. According to the accepted definition (11) that separates HKTs into two groups, we expected that a member of this family in rice, OsHKT2;4, would serve as a Na^+/K^+ symporter. To test this possibility, we performed an electrophysiological analysis of OsHKT2;4 in *Xenopus* oocytes. Applying the same conditions reported earlier (5), we recorded a OsHKT2;4 current using a two-electrode voltage-clamp protocol and uncovered an unanticipated current pattern (Fig. 1*A*). Oocytes injected with water ("Control" in Fig. 1) showed negligible current. However, oocytes expressing OsHKT2;4 generated currents that were large and time-dependent when applying highly hyperpolarized pulses. The current–voltage relationship displayed strong inward rectification with a profile reminiscent of numerous voltage-gated ion channels, including well-known K^+ channels in the *Shaker* family (16, 17). Also surprising was the tail current recorded at the 0 mV that displayed an initial rapid increase in amplitude followed by a slow decay (Fig. 1*A*). To amplify the tail current, a −120-mV prepulse was applied to elicit OsHKT2;4 activity followed by a succession of voltages ranging from −95 to −55 mV. The currents appeared to contain two components with different kinetics: one a slowly declining current observed at voltages more positive than 40 mV and the other rapidly activating with subsequent slowly deactivating currents appearing at voltages more negative than 10 mV (Fig. 1*B*). We suspected that these patterns likely emanated from the activation of endogenous channels in the oocytes. We thus decided to measure the activity of AtHKT1;1 as a control. As shown in Fig. 1*A*, the current generated by AtHKT1;1 was much smaller and displayed a time-independent "leak"-like current (Fig.1*A*) consistent with earlier results (18–21). Moreover, the tail currents of AtHKT1;1 also showed a time-independent leak profile (Fig.1*B*). To sum up, the results indicated that OsHKT2;4 produces a unique current profile that is absent in oocytes expressing other HKT members, including several previously described for rice (5, 6, 12–14).

Author contributions: W.-Z.L., W.W., H.-X.L., J.-P.G., and S.L. designed research; W.-Z.L., W.W., S.-M.W., J.-P.G., and L.-G.L. performed research; W.-Z.L., W.W., S.-M.W., B.B.B., H.-X.L., J.-P.G., and S.L. analyzed data; and W.-Z.L., B.B.B., J.P.-G., and S.L. wrote the paper.

The authors declare no conflict of interest.

[1]To whom correspondence may be addressed. E-mail: view@berkeley.edu or sluan@berkeley.edu.

This article contains supporting information online at www.pnas.org/cgi/content/full/1000698107/DCSupplemental.

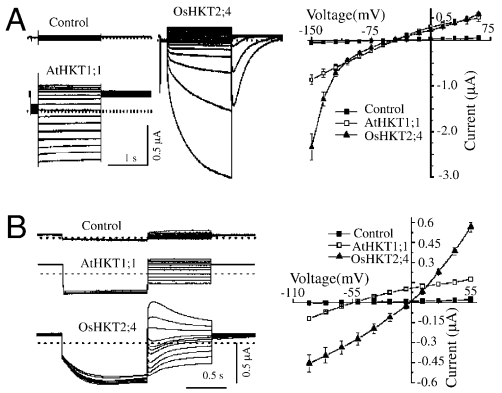

Fig. 1. Currents generated by AtHKT1;1 or OsHKT2;4 expressed in the *Xenopus* oocytes. (*A*) Time dependency and activation kinetics in the currents generated by OsHKT2;4. (*Left*) Typical whole-cell currents recorded by hyperpolarized pulses from the oocytes injected with water ("Control") or oocytes expressing AtHKT1;1 (AtHKT1;1) or OsHKT2;4 (OsHKT2;4) perfused with the bath solution containing (in mM) 0.3 K–gluconate, 10 Na–gluconate, 6 $MgCl_2$, 1.8 $CaCl_2$, 185 mannitol, and 10 Mes–Tris. Dotted lines represent the zero current level. The current–voltage relationships were deduced from 15 cells under each condition and presented on the right. (*B*) (*Left*) Traces show the typical tail currents generated by the control oocytes or oocytes expressing AtHKT1;1 or OsHKT2;4 recorded with the deactivation protocol. (*Right*) The current–voltage relationships were deduced from 12 cells/condition.

OsHKT2;4 Protein Constitutes a Ca^{2+}-Permeable, Nonselective Cation Channel. To assess the nature of OsHKT2;4 further, we first determined the ionic contribution to the currents by examining several cations present in the bath solution routinely used for HKT current analysis, namely, K^+, Na^+, Mg^{2+}, and Ca^{2+}. When perfused with only Na^+ or K^+ as the cation carrier, oocytes expressing OsHKT2;4 conducted current with both ions, but the currents were small compared to that observed with a mixture of the cations in the bath (Fig. 2 *A* and *B* and Fig. S1). In addition, the currents generated by K^+ or Na^+ alone, like that produced by AtHKT1;1, displayed typical leak-like patterns without significant time dependency (Fig. 2 *A* and *B*). Because the original bath solution contained (in mM) 6 Mg^{2+} and 1.8 Ca^{2+} in addition to 0.3 K^+ and 10 Na^+, we tested whether Mg^{2+} or Ca^{2+} functions as the cation carrier for the time-dependent current. Indeed, OsHKT2;4 conducted Mg^{2+} current as well. But again, the Mg^{2+} current was small compared with that with the mixed bath solution, and the current profile was different: both the Mg^{2+} current generated by highly hyperpolarized pulses (–120 and –150 mV) and the tail current displayed a weak time dependency (Fig. 2 *A* and *B* and Fig. S1).

When Ca^{2+} was added as the sole cation carrier in the perfusion solution, we compared the currents generated by a control oocyte with one expressing AtHKT1;1 and another expressing OsHKT2;4. The OsHKT2;4 current was significantly larger than those with other oocytes (Fig. 2*C*), and its reversal potential shifted to a more positive direction when the Ca^{2+} concentration was increased (Fig. 2*C*). By contrast, the reversal potentials from oocytes expressing AtHKT1;1 or OsHKT2;2 were insensitive to changes in extracellular Ca^{2+} concentration (Fig. S2). In addition, the presence of Ca^{2+} reduced OsHKT2;1-mediated Na currents, implying that Ca^{2+} may serve as a blocker of OsHKT2.1-mediated Na current (22). These results provided our first evidence that OsHKT2;4 functions as a Ca^{2+}-permeable channel.

The Ca^{2+} current generated with oocytes expressing OsHKT2;4 displayed two unique features: time dependency at hyperpolarization pulses and a highly active tail current similar to that recorded with a bath solution containing (in mM) 0.3 K^+, 10 Na^+, 1.8 Ca^{2+}, and 6 Mg^{2+} (Fig. 2 *A* and *B*). Removal of Ca^{2+} from the perfusion solution nearly eliminated these unique features and significantly reduced current magnitude (Fig. 2 *A* and *B*). To assess the relationship of cations in the bath solution, we recorded current in the presence of various combinations of these components. In each case, the currents appeared to be additive (Fig. S3). However, also in each case, the presence of Ca^{2+} was required for OsHKT2;4 to produce large, time-dependent currents with an active tail component. Furthermore, the presence of Ca^{2+} promoted inward rectification of the current whereas any combination of K^+, Na^+, and Mg^{2+} enhanced outward rectifying. The results suggested that Ca^{2+} determines the kinetics of currents generated by OsHKT2;4 in oocytes and that the presence of Ca^{2+} may enhance the influx of K^+, Na^+, and Mg^{2+} into plant cells.

The unique profiles observed with Ca^{2+} prompted the question whether the current responsible was due to an integral property of OsHKT2;4 or, alternatively, to endogenous oocyte channels activated by Ca^{2+} when OsHKT2;4 was expressed. It is well known that *Xenopus* oocytes have endogenous anion channels that are activated by intracellular Ca^{2+} (23, 24). It was, therefore, possible that OsHKT2;4 mediated Ca^{2+} entry and that this, in turn, activated endogenous anion channels. To test this possibility, we perfused with a solution containing Ca^{2+} salts of various anions, including 10 mM $CaCl_2$, CaI_2, Ca(gluconate)$_2$, and Ca$(NO_3)_2$. Interestingly, the amplitude and reversal potentials of currents recorded under hyperpolarized pulses were similar irrespective of the anion species (Fig. 3*A*). The tail currents recorded at various voltages after a –120-mV prepulse, however, exhibited different permeability with the sequence of $NO_3^- > I^- > Cl^- >$ gluconate$^-$ (Fig. 3*A*). These results suggested that currents produced by hyperpolarization were not anion currents, but, rather, that the tail currents were carried by anions. The fact that only Ca^{2+} produced a unique tail current (Fig. 2 and Fig. S3) suggests that this current was activated upon Ca^{2+} entry.

To test this possibility, the amplitude and reversal potentials of currents were determined with OsHKT2;4-injected oocytes perfused with a solution containing $CaCl_2$ with or without Na_4–EGTA. Because EGTA is a Ca^{2+} chelator, its addition reduces free Ca^{2+} but does not change Cl^- concentration. The amplitude of the hyperpolarization-activated currents and the tail currents were eliminated by the addition of EGTA and were then similar to those observed with EGTA alone (Fig. 3*B*). These results are consistent with the conclusion that the hyperpolarization-activated current was carried by Ca^{2+}, whereas the active tail current was an anion current that required Ca^{2+} influx.

To confirm further that OsHKT2;4 facilitates Ca^{2+} influx, we performed a direct Ca^{2+} ($^{45}Ca^{2+}$) uptake assay using oocytes expressing OsHKT2;4. As shown in Fig. 3*C*, the oocytes expressing OsHKT2;4 showed a significantly higher rate of $^{45}Ca^{2+}$ accumulation relative to the control oocytes, in both a time- and concentration-dependent manner, supporting the conclusion that OsHKT2;4 functions as a Ca^{2+} channel.

Taken together, the above results indicate that the Ca^{2+}-current generated by OsHKT2;4 consists of two components: a hyperpolarization-activated current carried by Ca^{2+} and an endogenous Ca^{2+}-activated anion tail current. Indeed, an outward-rectifying, Ca^{2+}-activated Cl^- channel (CaCC) was recently cloned from *Xenopus* oocytes with the same sequence of anion permeability seen in Fig. 3*A*. The channel is effectively inhibited by 0.1 mM 4,4′-diisothiocyanostilbene-2,2′-disulfonic acid (DIDS), niflumic acid (NFA), 5-nitro-2-(3-phenylpropylalanine) benzoate (NPPB), and tamoxifen (25). We therefore added these inhibitors (at 0.1 mM) to the 10-mM Ca^{2+} perfusion solution bathing the OsHKT2;4 oocytes. The inhibitors failed to affect the currents recorded at hyperpolarized pulses [Fig. 3*D* (*i*)], but they clearly inhibited the tail current and shifted the reversal potential to a more negative voltage [Fig. 3*D* (*ii* and *iii*)]. The results further support the hypothesis that OsHKT2;4 expressed in *Xenopus* oocytes conducts an inward Ca^{2+} current at hyperpolarization

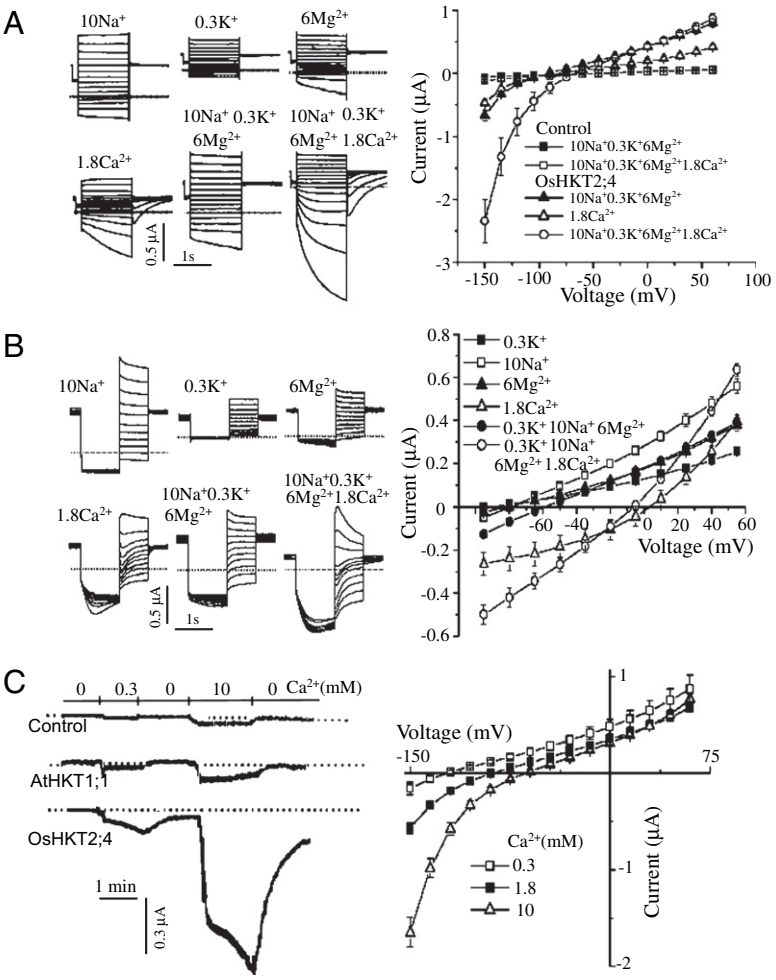

Fig. 2. Ca^{2+} determines the kinetics of OsHKT2;4 currents. (*A*) Ca^{2+} induced the time dependency and large magnitude in the current recorded by hyperpolarized pulses. The typical current traces were generated by the oocytes expressing OsHKT2;4 perfused with various ions (*Left*). The mean current data were deduced from the recordings of the control oocytes and the oocytes expressing OsHKT2;4 perfused by the buffer solution containing (in mM) 10 Na^+ + 0.3 K^+ + 6 Mg^{2+}, 10 Na^+ + 0.3 K^+ + 6 Mg^{2+} + 1.8 Ca^{2+}, or 1.8 Ca^{2+} (*Right*). (*B*) Unique tail currents induced by Ca^{2+}. (*Left*) Traces show the typical tail currents generated by oocytes expressing OsHKT2;4 perfused with various ions. (*Right*) The mean tail currents were summarized from recordings of the oocytes expressing OsHKT2;4 perfused with the solution containing (in mM) 10 Na^+, 0.3 K^+, 6 Mg^{2+}, and 1.8 Ca^{2+}, 10 Na^+ + 0.3 K^+ + 6 Mg^{2+}, or 10 Na^+ + 0.3 K^+ + 6 Mg^{2+} + 1.8 Ca^{2+}. (*C*) The OsHKT2;4 current was sensitive to extracellular Ca^{2+} concentration. (*Left*) The typical current traces were recorded at −120 mV from the control oocyte and the oocyte expressing AtHKT1;1 or OsHKT2;4 perfused with a solution containing (in mM) 185 mannitol and 10 Mes–Tris (pH 7.4) with 0, 0.3, or 10 Ca^{2+}. (*Right*) The current–voltage relationship was deduced from recordings of the oocytes expressing OsHKT2;4. Summarized current data are from 10 cells/condition.

pulses, leading to the activation of an endogenous CaCC. Although we cannot completely rule out the possibility that OsHKT2;4 produces the anion tail current, it is very unlikely for the cation channel to conduct an anion tail current.

We tested several other cations and found that HKT2;4 was permeable to a broad range of monovalent and divalent species (Fig. 4*A*). Compared with the control, OsHKT2;4 conducted current carried by NH_4^+, Li^+, Na^+, or K^+, whereas AtHKT1;1 was sensitive mainly to Na^+ [Fig.4*A* (*i*)]. OsHKT2;4 was significantly permeable to Ca^{2+}, Mg^{2+}, Zn^{2+}, Mn^{2+}, Cu^{2+}, Fe^{2+}, and Cd^{2+} relative to the control [Fig. 4*A* (*ii*)]. Among the cations, Ca^{2+} was most permeable. Moreover, aside from Ca^{2+}, none of the cations produced unique tail currents, thus providing additional evidence that the tail current was Ca^{2+} dependent. We also tested trivalent cations such as La^{3+}, Gd^{3+}, and Al^{3+}, but none produced significant current [Fig. 4*A* (*iii*)].

To assess the channel properties of OsHKT2;4 further, we performed patch-clamp recordings using excised inside-out patches. Single-channel current analysis showed that the protein acted as a bona fide channel with a conductance of 4.5 ± 0.5 pA and an open probability of 54 ± 4 at a membrane potential of 150 mV (Fig. 4*C*). Although OsHKT2;4 lacks voltage sensors in its transmembrane segments, the open probability appears to be voltage-dependent (Fig. 4*C*). This type of activation may result from a concerted conformational change at the selectivity filters that contributes to voltage-dependent gating of KcsA (26, 27). Indeed, the selectivity filters in the HKT protein family are structurally related to those of KcsA (19). Recently, another HKT, OsHKT1;1 expressed in oocytes, produced currents with voltage-dependent properties recorded upon hyperpolarized pulses (6), thus further supporting the view that HKT family members are, indeed, voltage-regulated channels.

OsHKT2;4 Protein May Constitute Two Separate Conducting Pathways. The current profile of OsHKT2;4 is similar to that of certain other nonselective cation channels. Its structure, however, appears to have evolved from KcsA, a typical K^+-selective channel (9, 10, 19). We entertained the idea that OsHKT2;4, unlike a regular symporter, may indeed function as a bona fide ion channel. On the basis of its broad range of ion permeability, this channel may behave differently from a typical K^+-selective or Ca^{2+}-selective channel. We therefore tested whether OsHKT2;4 is sensitive to blockers typical of K^+ and Ca^{2+} channels. Interestingly, the OsHKT2;4 current was blocked by Ba^{2+}, a typical K^+-channel blocker, only when K^+ or Na^+ was used as a carrier, not with Ca^{2+} [Fig. 4*B* (*i*)]. Further, we found that Ca^{2+}-channel blockers such as La^{3+} and Gd^{3+}, but not Ba^{2+}, blocked the OsHKT2;4 activity when Ca^{2+} was used as a conducting ion [Fig. 4*B* (*ii*)]. We also measured the effect of these Ca^{2+} channel blockers in a $^{45}Ca^{2+}$ uptake assay and found that the presence of La^{3+} or Gd^{3+} almost completely blocked $^{45}Ca^{2+}$ accumulation in the oocytes [Fig. 4*B* (*iii*)].

It is intriguing that the Mg^{2+} current was partially blocked by either La^{3+} or Ba^{2+} [Fig. 4*B* (*i*)], indicating that Mg^{2+} conductance shares a common path with Ca^{2+} and K^+. Collectively, these results suggest that HKT2;4 may have at least two "pathways" (or binding sites) for cation transport: one for smaller cations such as Na^+ and K^+ and the other for larger divalent

PLANT BIOLOGY

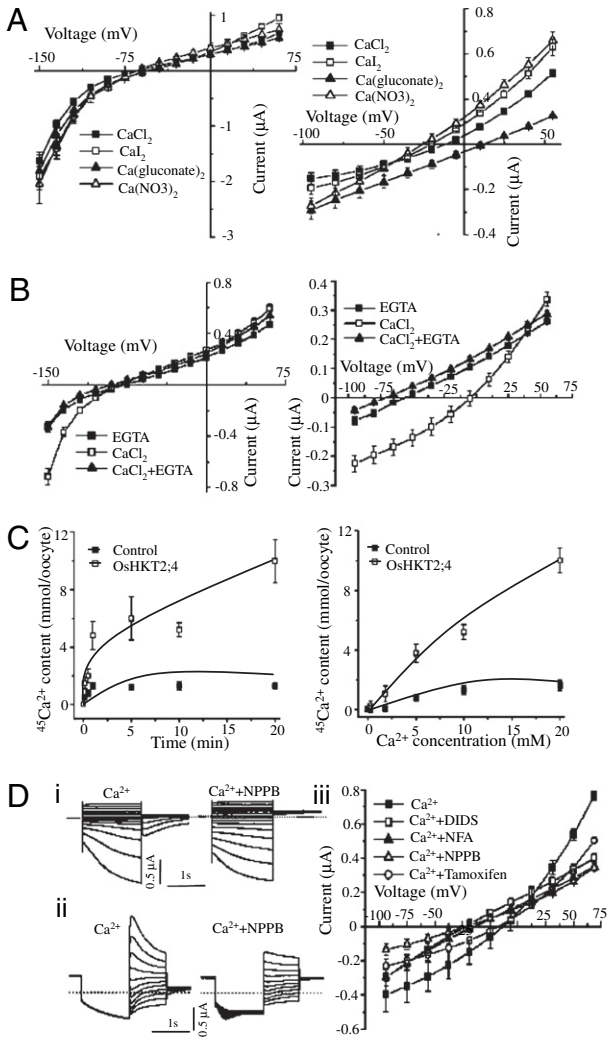

Fig. 3. OsHKT2;4 expression facilitates Ca^{2+} accumulation in *Xenopus* oocytes. (*A*) The hyperpolarized pulses produced the same current in the OsHKT2;4-injected oocytes perfused by different Ca^{2+} salts (*Left*). But the tail current recorded under voltage steps of 55 to −95 mV following a prepulse at −120 mV was dependent on the anions in the Ca^{2+} salts (*Right*). The oocytes were perfused with a solution containing (in mM) 185 mannitol and 10 Mes–Tris with 10 $CaCl_2$, CaI_2, Ca $(gluconate)_2$, or $Ca(NO_3)_2$. (*B*) The current–voltage relationship was deduced from currents recorded by hyperpolarized pulses (*Left*) or by deactivation protocol (*Right*), respectively. The oocytes were perfused with a solution containing (in mM) 185 mannitol and 10 Mes–Tris with 5 EGTA–Na_4, 1.8 $CaCl_2$, or 1.8 $CaCl_2$ + 5 EGTA. (*C*) OsHKT2;4-injected oocytes uptake more Ca^{2+} than control oocytes. (*Left*) The time course of $^{45}Ca^{2+}$ accumulation in oocytes bathed in 1.8 mM $CaCl_2$. (*Right*) The concentration-dependent $^{45}Ca^{2+}$ accumulation in the oocytes incubated for 10 min in a solution containing 0, 0.3, 1.8, 5, 10, or 20 mM $CaCl_2$. (*D*) The typical traces of the currents recorded by hyperpolarized pulses (*i*) or the tail currents (*ii*) in OsHKT2;4-injected oocytes perfused with the solution containing (in mM) 10 $CaCl_2$ or 10 $CaCl_2$ + 0.1 NPPB. (*iii*) The current–voltage relationship was deduced from the tail current recorded from OsHKT2;4-injected oocytes perfused with the same solution containing various inhibitors, including 0.1 mM of DIDS, NFA, NPPB, or tamoxifen. Summarized Ca^{2+} uptake was deduced from results of 50 oocytes/condition repeated in three separate experiments, and the current data are from 10 cells/condition.

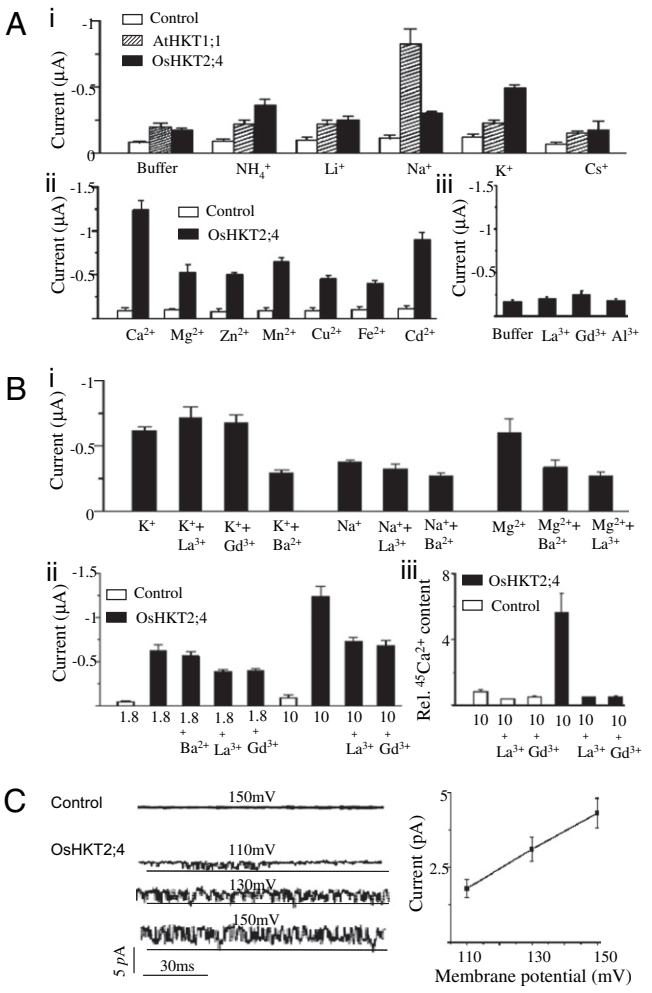

Fig. 4. OsHKT2;4 functions as a nonselective cation channel with multiple pathways. (*A*) OsHKT2;4 expressed in the oocytes was permeable to a broad range of cations. (*i*) The currents at −150 mV recorded from the control oocytes or the oocytes expressing AtHKT1;1 or OsHKT2;4 perfused with a solution containing 185 mM mannitol, 10 mM Mes–Tris ("Buffer"), or the same "Buffer" with 10 mM NH_4^+, Li^+, Na^+, K^+, or Cs^+. (*ii*) The mean current at −150 mV recorded from the control oocytes or the oocytes expressing OsHKT2;4 perfused with the same "Buffer" containing 10 mM Ca^{2+}, Mg^{2+}, Zn^{2+}, Mn^{2+}, Cu^{2+}, Fe^{2+}, or Cd^{2+}. (*iii*) The mean currents at −150 mV recorded from the oocytes expressing OsHKT2;4 perfused with the "Buffer" or Buffer plus 1 mM La^{3+}, Gd^{3+}, or Al^{3+}. (*B*) The activity of OsHKT2;4 was inhibited by the channel blockers. (*i*) The mean current at −150 mV recorded from the oocytes expressing OsHKT2;4 perfused with a "Buffer" containing (in mM) 10 K^+ + 1 La^{3+}, 10 K^+ + 1 Gd^{3+}, 10 K^+ + 1 Ba^{2+}, 10 Na^+, 10 Na^+ + 1 La^{3+}, 10 K^+ + 1 Ba^{2+}, 10 Mg^{2+}, 10 Mg^{2+} + 1 Ba^{2+}, or 10 Mg^{2+} + 1 La^{3+}. (*ii*) The mean current at −150 mV recorded with control oocytes or oocytes expressing OsHKT2;4 perfused with a "Buffer" containing either 1.8 or 10 mM Ca^{2+} in the presence or absence of 1 mM indicated blocker. (*iii*) $^{45}Ca^{2+}$ accumulation in control oocytes expressing OsHKT2;4, incubated in a "Buffer" with (in mM) 10 Ca^{2+}, 10 Ca^{2+} + 1 La^{3+} or 10 Ca^{2+} + 1 Gd^{3+} for 10 min. The relative $^{45}Ca^{2+}$ content in the oocytes was calculated as the ratio of $^{45}Ca^{2+}$ accumulation in the OsHKT2;4-injected oocytes over control oocytes in the presence of 10 mM Ca^{2+}. (*C*) OsHKT2;4 activity recorded from excised inside-out patches of the oocytes. (*Left*) Representative currents in an excised inside-out patch recorded at membrane potentials of 110, 130, or 150 mV. The horizontal line represents the zero current level. (*Right*) Current–voltage relationship of currents from excised inside-out patches. Summarized Ca^{2+} uptake was deduced from results of 50 oocytes/condition repeated in three separate experiments, and the current recording data are from 10 cells/condition.

cations such as Ca^{2+}. Mg^{2+} may be able to proceed via either pathway on the basis of inhibitor analysis.

OsHKT2;4 Protein Is Localized to the Plasma Membrane and Likely Facilitates Cation Uptake by Plants. To probe its physiological function, we examined the expression pattern and subcellular localization of OsHKT2;4 in rice plants. We first examined tissue localization of *OsHKT2;4* mRNA with RT–PCR and found the

gene expressed in spikelets, leaves, leaf sheathes, internodes, nodes, the base of stems, and roots (Fig. 5*A*). We also produced transgenic rice plants transformed with an *OsHKT2;4* promoter–β-glucuronidase (GUS) reporter gene and examined the cell-type-specific pattern of GUS activity by histochemical staining. Strong GUS expression was observed in the vasculature of spikelets [Fig. 5*B* (*a*)], leaves [Fig. 5*B* (*c*, *d*, and *f*)], leaf sheaths [Fig. 5*B* (*e* and *f*)], stems [Fig. 5*B* (*j*, *k*, *i*, and *n*)], leaf epidermal cells [Fig. 5*B* (*b*)], and primary [Fig. 5*B* (*g* and *m*)] and lateral roots [Fig. 5*B* (*g*, *l*, and *h*)]. Weak GUS staining was also observed in other tissues, such as mesophyll cells [Fig. 5*B* (*b*)]. In contrast to OsHKT1;5 and AtHKT1;1 that were expressed mainly in vascular tissues (5, 28), the diverse expression pattern of OsHKT2;4 resembled closely that of other group 2 members, including TaHKT2;1, OsHKT2;1, and OsHKT2;2 (7, 29).

Subcellular localization determines the cellular function of a transporter. A previous study concluded that AtHKT1;1 is localized in the plasma membrane of xylem parenchyma cells (28), thus indicating a role in retrieval of Na^+ from xylem vessels. For subcellular localization of the OsHKT2;4, we generated specific antibodies against the protein and then applied immunogold labeling coupled with electron microscopic analysis. A short peptide, PSMNSTDIKRSCHK, corresponding to amino acids 150–163, was selected as the antigenic epitope. Because OsHKT2;3 is highly homologous to OsHKT2;4, Western blot analysis was carried out to confirm that the antibody was specific for OsHKT2;4 and did not react with OsHKT2;3 (Fig. S4). As seen in Fig. 5, OsHKT2;4 was observed earlier in tissues shown to express the promoter–GUS reporter. In the root-hair cross-section, the gold particles were enriched at the cell surface, likely the plasma membrane [Fig. 5*C* (*b* and *c*)]. The same localization pattern was observed with sections of other cell types, including epidermal cells of leaves and vascular tissues of roots and leaves (Fig. S4). The results are consistent with the conclusion that OsHKT2;4 is localized to the plasma membrane.

On the basis of its expression pattern and subcellular localization, OsHKT2;4 acts as a plasma membrane transporter to facilitate the influx and efflux of cations. With Ca^{2+}, the direction of cation transport is mainly inward rectifying. We also attempted to discern the function of OsHKT2;4 by genetic analysis. We began by isolating several homozygous lines of *Tos*-tagged *Oshkt2;4* mutants and by characterizing their phenotypes. The mutants, however, behaved similarly to wild-type plants under both normal and salt stress conditions (Fig. S5). Further, they contained a similar content of cations, including Na^+, K^+, Mg^{2+}, Ca^{2+}, and others as determined by the inductively coupled plasma analysis. The absence of a phenotypic change in the mutants suggests that OsHKT2;4 is functionally redundant with other transporters. Indeed, another HKT family member encoded in the rice genome, OsHKT2;3, is more than 90% identical to OsHKT2;4 at the amino acid level. This and possibly other transporters may function in the same manner as OsHKT2;4, thus preventing phenotypic change following disruption of the relevant gene.

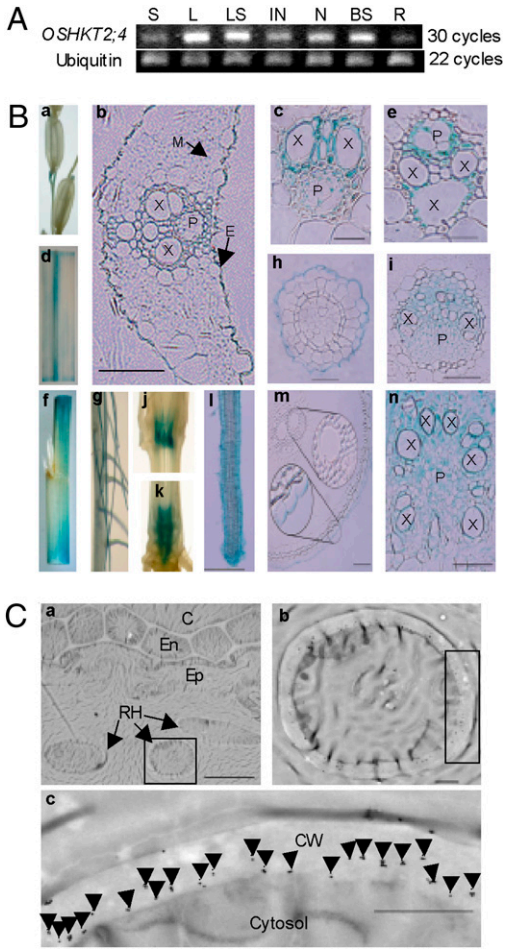

Fig. 5. Expression pattern and subcellular localization of OsHKT2;4 protein. (*A*) Expression of *OsHKT2;4* analyzed using RT–PCR in various organs of the Nipponbare plant. Ubiquitin was used as a control. S, spikelet; L, leaf; LS, leaf sheath; IN, internode; N, node; BS, base of stem; R, root. (*B*) In *OsHKT2;4* promoter–GUS transgenic plants, GUS was expressed in spikelets (*a*), leaves (*d* and *f*), leaf sheaths (*f*), nodes (*j* and *k*), internodes (*k*), primary roots (*m*) and lateral roots (*g* and *l*), cross-sections of leaves (*b*), main veins of leaves (*c*), leaf sheaths (*e*), nodes (*i*), base of stems (*n*), primary roots (*h*), and lateral roots (*h*). E, epidermis; M, mesophyll; X, xylem; P, phloem. (Scale bars: *c*, *e*, and *h*—20 μm; *b*, *i*, *l*, *m*, and *n*—50 μm.) (*C*) Immunogold localization of the OsHKT2;4 protein to the plasma membrane of root hair cells. *b* and *c* are enlarged sections of *a*. Arrows indicate gold particles. RH, root hair; Ep, epidermis; En, endodermis; C, cortex; CW, cell wall. (Scale bars: *a*, 10 μm; *b* and *c*, 1 μm.)

Concluding Remarks

Although related to high-affinity K^+ transporters in bacteria and fungi, several studies have concluded that HKT proteins in plants function as Na^+ uniporters or Na^+–K^+ symporters consistent with the acquisition of structural and functional diversity during evolution. Interestingly, even among flowering plants, HKT proteins appear to have evolved rapidly. Thus, *Arabidopsis*, a model dicot, differs markedly from rice, a model monocot. Whereas the *Arabidopsis* genome contains a single *HKT* gene, rice contains up to nine *HKT* genes (depending on variety). However, despite the presence of more family members, rice HKT proteins are highly similar in their amino acid sequences, suggesting structural and functional similarities. Indeed, consistent with earlier work on AtHKT1;1 and wheat HKT1, studies conducted so far have defined rice HKT proteins as Na^+ uniporters or Na^+–K^+ symporters.

The experiments described here, surprisingly, have revealed a distinct feature of the rice HKT member, OsHKT2;4—i.e., that it functions as a Ca^{2+}-permeable, nonselective cation channel. This feature underscores the structural and functional diversity of plant HKT proteins and extends their function to the previously unknown Ca^{2+} arena. Because Ca^{2+}-permeable channels function in controlling Ca^{2+} flux, HKT proteins likely also link Ca^{2+} to the regulation of signal transduction via its role as second messenger (30). In this regard, HKT members involved in calcium signaling may be a fundamental divergence of function between dicot and monocot HKT proteins. Likewise, the evolutionary divergence of the dicot and monocot HKTs may have potential implications in the divergence of the adaptive properties of these plants species, including adaptation to various environmental conditions.

Considering its potential role in Ca^{2+} signaling and nutrient uptake, OsHKT2;4 may be essential for plant growth and development, especially under stress conditions. Disruption of OsHKT2;4 expression in rice failed, however, to affect plant growth and development under normal as well as stress conditions. This finding underscores the need to examine the potential functional redundancy between OsHKT2;4 and similar proteins in the HKT family as well as between proteins in other families with similar functions. Elucidation of the functional relationships among these different membrane proteins should enhance our understanding of the regulation of Ca^{2+} fluctuation and homeostasis in plant cells.

Materials and Methods

RNA Extraction and Transcript Analysis. Total RNA extraction and the first-strand cDNA synthesis were done as described previously (5). The OsHKT2;4 transcripts were detected by PCR under the following program: 94 °C for 5 min; 30 cycles of 94 °C for 15 s, 56 °C for 15 s, and 72 °C for 40 s; and 72 °C for 10 min. The rice ubiquitin cDNA served as an endogenous control.

***OsHKT2;4* Promoter–GUS Analysis.** A 1920-bp *OsHKT2;4* promoter region upstream of the initial ATG codon was amplified from Nipponbare genomic DNA. The fusion construct of the promoter–GUS reporter, generation of transgenic plants carrying this construct, and GUS histochemical analysis were done as described previously (5).

Immunogold Detection. A 14-residue peptide, PSMNSTDIKRSCHK, corresponding to the amino acid position 150–163 of OsHKT2;4, was synthesized as an epitope to produce rabbit antiserum containing the anti-OsHKT2;4 antibodies. Ten-nanometer, gold-conjugated, goat anti-rabbit IgGs were used as the secondary antibodies. Specimens from 10-day-old Nipponbare seedlings were trimmed to 1 mm^2. Osmium tetroxide fixation, thin sectioning, immunogold labeling, and electron microscopy were carried out as described (31).

$^{45}Ca^{2+}$ Uptake Assay in the Oocytes. Fifty oocytes were placed as a group into a solution containing (in mM) 10 Mes–Tris and 185 mannitol, pH 7.4, with various concentrations of $CaCl_2$ supplemented with 25 KBq/mL $^{45}Ca^{2+}$. Every 10 oocytes were grouped in one scintillation counting vial, incubated with a 2-mL mixture solution supplemented with 0.5 mL 10% SDS overnight, and counted with a liquid scintillation counter.

Electrophysiological Analysis. Freshly isolated *Xenopus* oocytes were injected with 23 nL of 500 μg/mL cRNA and used for voltage-clamp experiments 2 days after injection. Unless otherwise indicated, the perfusion solution and pipette solution used in the two-electrode voltage clamp recordings were as previously described (5). The perfusion solution contained (in mM) 0.3 K–gluconate, 10 Na–gluconate, 6 $MgCl_2$, 1.8 $CaCl_2$, 185 mannitol, and 10 Mes–Tris (pH 7.4). The current was record by hyperpolarized pulses of a 0.2-s prepulse at −40 mV followed by voltage steps of 60 to −150 mV (in 15 mV decrements, 1.8-s duration) followed by a 1.5-s deactivation at 0 mV. The deactivation protocol of a 1.33-s prepulse at −120 mV was followed by stepping to voltages ranging 55 to −95 mV (in 15 mV decrements, 1-s duration) to amplify the tail currents. The bath solution was used in the excised inside-out patch recordings containing (in mM) 1 $CaCl_2$, 0.1 DIDS, and 10 Mes–Tris (pH 7.4). The pipette solution consisted of (in mM) 10 $CaCl_2$, 0.1 DIDS, 10 Mes–Tris (pH 7.4). The summarized data of the currents recorded under hyperpolarization and the tail currents shown in Figs. 1–4 were generated from the pooled currents at 2 or 1.8 s for each voltage-clamp episode, respectively. Data in Figs. 1–4 are presented as representative recordings or as mean ± SE of n observations with three repetitions, in which n is the number of samples. Statistical comparisons were made using unpaired t tests as appropriate, and differences were considered to be significant at $P < 0.05$.

ACKNOWLEDGMENTS. We thank Dr. E. Y. Isacoff for providing oocytes used in this study. This research was supported by the National Science Foundation, the US Department of Agriculture (S.L. and B.B.B.), the National Natural Science Foundation of China (30771158, 30830070), and the Ministry of Agriculture of China (2008ZX08009-003, 2009ZX08009-127).

1. Nakamura T, Yuda R, Unemoto T, Bakker EP (1998) KtrAB, a new type of bacterial K^+-uptake system from *Vibrio alginolyticus*.. *J Bacteriol* 180:3491–3494.
2. Gaber RF, Styles CA, Fink GR (1988) TRK1 encodes a plasma membrane protein required for high-affinity potassium transport in *Saccharomyces cerevisiae*. *Mol Cell Biol* 8:2848–2859.
3. Ko CH, Gaber RF (1991) TRK1 and TRK2 encode structurally related K^+ transporters in *Saccharomyces cerevisiae*. *Mol Cell Biol* 11:4266–4273.
4. Gassmann W, Rubio F, Schroeder JI (1996) Alkali cation selectivity of the wheat root high-affinity potassium transporter HKT1. *Plant J* 10:869–882.
5. Ren ZH, et al. (2005) A rice quantitative trait locus for salt tolerance encodes a sodium transporter. *Nat Genet* 37:1141–1146.
6. Jabnoune M, et al. (2009) Diversity in expression patterns and functional properties in the rice Hkt transporter family. *Plant Physiol* 150:1955–1971.
7. Schachtman DP, Schroeder JI (1994) Structure and transport mechanism of a high-affinity potassium uptake transporter from higher plants. *Nature* 370:655–658.
8. Horie T, Hauser F, Schroeder JI (2009) HKT transporter-mediated salinity resistance mechanisms in Arabidopsis and monocot crop plants. *Trends Plant Sci* 14:660–668.
9. Durell SR, Guy HR (1999) Structural models of the KtrB, TrkH, and Trk1,2 symporters based on the structure of the KcsA K^+ channel. *Biophys J* 77:789–807.
10. Kato Y, et al. (2001) Evidence in support of a four transmembrane-pore-transmembrane topology model for the *Arabidopsis thaliana* Na^+/K^+ translocating AtHKT1 protein, a member of the superfamily of K^+ transporters. *Proc Natl Acad Sci USA* 98:6488–6493.
11. Platten JD, et al. (2006) Nomenclature for HKT transporters, Key determinants of plant salinity tolerance. *Trends Plant Sci* 11:372–374.
12. Garciadeblas B, Senn ME, Banuelos MA, Rodriguez-Navarro A (2003) Sodium transport and HKT transporters: The rice model. *Plant J* 34:788–801.
13. Horie T, et al. (2001) Two types of HKT transporters with different properties of Na^+ and K^+ transport in *Oryza* sativa. *Plant J* 27:129–138.
14. Golldack D, et al. (2002) Characterization of a HKT-type transporter in rice as a general alkali cation transporter. *Plant J* 31:529–542.
15. Horie T, et al. (2007) Rice OsHKT2;1 transporter mediates large Na^+ influx component into K^+-starved roots for growth. *EMBO J* 26:3003–3014.
16. Ward JM, Maser P, Schroeder JI (2009) Plant ion channels: Gene families, physiology, and functional genomics analyses. *Annu Rev Physiol* 71:59–82.
17. Lebaudy A, Very AA, Sentenac H (2007) K^+ channel activity in plants: Genes, regulations and functions. *FEBS Lett* 581:2357–2366.
18. Uozumi N, et al. (2000) The *Arabidopsis* HKT1 gene homolog mediates inward Na^+ currents in *Xenopus laevis* oocytes and Na^+ uptake in *Saccharomyces cerevisiae*. *Plant Physiol* 122:1249–1259.
19. Maser P, et al. (2002) Glycine residues in potassium channel-like selectivity filters determine potassium selectivity in four-loop-per-subunit HKT transporters from plants. *Proc Natl Acad Sci USA* 99:6428–6433.
20. Kato N, et al. (2007) Role of positively charged amino acids in the M2D transmembrane helix of Ktr/Trk/HKT type cation transporters. *Channels* 1:161–171.
21. Berthomieu P, et al. (2003) Functional analysis of AtHKT1 in *Arabidopsis* shows that Na^+ recirculation by the phloem is crucial for salt tolerance. *EMBO J* 22:2004–2014.
22. Yao X, et al. (2010) Differential sodium and potassium transport selectivities of the rice OsHKT2;1 and OsHKT2;2 transporters in plant cells. *Plant Physiol* 152:342–355.
23. Barish ME (1983) A transient calcium-dependent chloride current in the immature *Xenopus* oocyte. *J Physiol* 342:309–325.
24. Hartzell C, Putzier I, Arreola J (2005) Calcium-activated chloride channels. *Annu Rev Physiol* 67:719–758.
25. Schroeder BC, Cheng T, Jan YN, Jan LY (2008) Expression cloning of TMEM16A as a calcium-activated chloride channel subunit. *Cell* 134:1019–1029.
26. Cordero-Morales JF, Cuello LG, Perozo E (2006) Voltage-dependent gating at the KcsA selectivity filter. *Nat Struct Mol Biol* 13:319–322.
27. Cordero-Morales JF, et al. (2006) Molecular determinants of gating at the potassium-channel selectivity filter. *Nat Struct Mol Biol* 13:311–318.
28. Sunarpi, et al. (2005) Enhanced salt tolerance mediated by AtHKT1 transporter-induced Na^+ unloading from xylem vessels to xylem parenchyma cells. *Plant J* 44: 928–938.
29. Kader MA, Seidel T, Golldack D, Lindberg S (2006) Expressions of OsHKT1, OsHKT2, and OsVHA are differentially regulated under NaCl stress in salt-sensitive and salt-tolerant rice (*Oryza sativa* L.) cultivars. *J Exp Bot* 57:4257–4268.
30. Luan S, Kudla J, Rodriguez-Concepcion M, Yalovsky S, Gruissem W (2002) Calmodulins and calcineurin B-like proteins: calcium sensors for specific signal response coupling in plants. *Plant Cell* 14(Suppl):S389–S400.
31. Alcantara J, Bird DA, Franceschi VR, Facchini PJ (2005) Sanguinarine biosynthesis is associated with the endoplasmic reticulum in cultured opium poppy cells after elicitor treatment. *Plant Physiol* 138:173–183.